Galactic Cosmic Rays induced Radiation Environment at the surface of Mars

Keating A., Pimenta M., Mohammadzade A., Nieminen P., Daly E.

***Abstract*— MarsREC, a modelling framework for Mars Radiation Environment Characterization and effects was developed. MarsREC allows the investigation of the radiation environment at the surface of Mars, including input solar cycle modulated cosmic ray and solar particles from CREME-96 and transport of radiation in the Martian atmosphere and regolith using Geant4 Monte-Carlo toolkit. In this poster we investigate the radiation environment at the surface of Mars due to Galactic Cosmic Rays fluxes.**

***Index Terms*— MarsREC, Mars, Radiation Environment, GEANT4, Galactic Cosmic Rays**

I. Introduction

When planning spacecraft and manned missions to Mars, detailed information about environmental conditions and radiation on the planet is vital to reduce the chances of mission failure and to aid in the optimisation of the design process.

While there are some similarities with the Earth's radiation environment, each planet has important unique features.

A quantitative description of the radiation environment of Mars in terms of particle species and energy spectra relies on the careful modelling of a) atmosphere climatic variables (pressure, temperature, density, composition, dust storms); b) local geology/topology; c) distance from the Sun and d) any local magnetosphere [1][3].

A modelling framework for the prediction of the framework for Mars Radiation Environment Characterization and induced Effects was developed. MarsREC features include input solar cycle modulated cosmic ray and solar particle event spectra, both based on CREME-96, the transport of this radiation in the Martian atmosphere and regolith, including creation of secondary radiation, using the Geant4 Monte-Carlo toolkit [4][5].

Details of the atmosphere are derived from the European Mars Climate Database (EMCD) with a dense topological grid and layering of the atmosphere [1][2][6][7]. Seasonal and diurnal variations are considered for different location. Surface topology is derived from the Mars Orbiter laser altimeter (MOLA) and geology is modeled. The outputs are full energetic particle transport histories, maps of radiation fluxes and doses.

The Martian climatological fields (atmospheric temperature, water column density) vary strongly with season, local time, and location.

In this paper we focus on the characterization of the galactic cosmic rays induced radiation environment at the surface of Mars and its variation with seasonal atmospheric changes. Moreover galactic cosmic rays induced effects are evaluated and compared with other software results.

A. Input radiation

In interplanetary space the radiation sources are solar X-rays, Solar Energetic Particles (SEP), consisting of protons and other ions, energetic electrons originating in Jupiter's magnetosphere, Galactic Cosmic Rays (GCR) and galactic X-rays and gamma rays. However, for Mars-orbiting and landing missions the radiation environment is mainly due to GCR and SEP [1][2].

Although SEP the interplanetary transport may be very complex and dependent on many factors such as energy, time, and solar wind conditions, GCR fluxes may not vary significantly from near-Earth interplanetary locations to Mars [10] [11].

In this paper the GCR input fluxes was considered for the "maximum" phase of the solar cycle, but with "quiet" interplanetary conditions. The inputs were derived from the CREME96 model [10][11]. This model represents the environment that prevails in the absence of solar energetic particle events for near-Earth interplanetary locations. These interplanetary flux models are based on measurements at Earth (1AU[1]). Its intensity varies over a 22-years solar cycle. The phasing with respect to the solar cycle corresponds to the foreseen European Mars mission ExoMars [12] expected to be launched in 2011.

B. European Mars Climate Database [6][7]

The EMCD contains data such as temperature, wind, density, pressure, among other parameters, resulting from global circulation model simulations, stored on a accurate longitude-latitude grid from the surface up to an altitude of approximately a few hundreds of kilometers from the surface. Altitudes can be defined with respect to local topological elevations.

The vertical coordinate for the 3D spatial variables is defined as $\sigma = p/p_0$, where p is the atmospheric pressure and p_0 is the local surface pressure, also stored in the database. Thus, σ is 1 at the surface and 0 at infinity and the σ levels follow the model topography. Depending on the EMCD version there are 32 to 50 σ levels delineating atmospheric layers.

Wind, temperature, pressure and other fields are averaged and stored for 12 Martian Universal Times at longitude 0^o, for 12

[1] Medium Earth-Sun distance corresponds to approximately 150×10^6 km.

Martian "seasons" to give a comprehensive representation of the annual and diurnal cycles.
An interface has been built in order to read EMCD data as input for the Geant4 simulation Geometry Construction class, for each location, time and solar longitude.
Figure 1 illustrates the different Martian seasons and solar longitude variation.

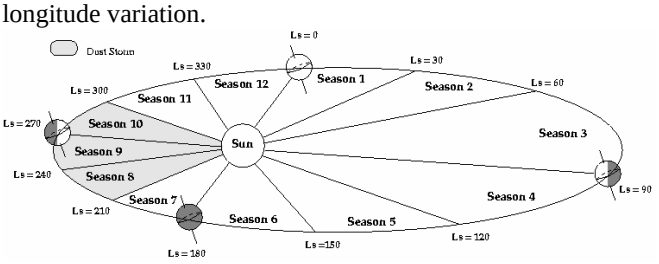

Figure 1- Representation of twelve typical Martian seasons according to EMCD.

Figure 2 shows the EMCD Viking dust scenario daily-averaged pressure from the Viking sites. An estimate of the variability due to weather systems, with the seasonal trend component of the EMCD variance removed, is also shown. The seasonal cycle is due largely to the condensation and sublimation of CO_2, although there is an important dynamical component [7], while the high-frequency oscillations are due to weather systems passing over the Landers [7].

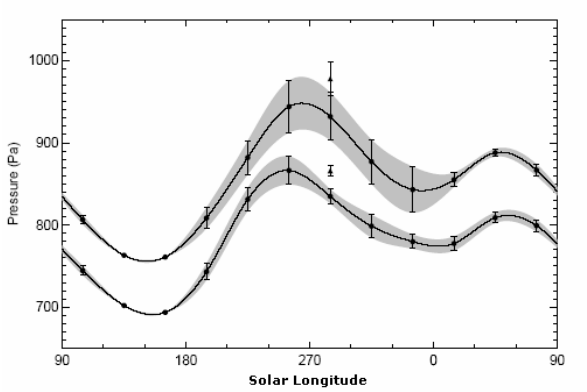

Figure 2 - Pressure at the Viking 1[2] (bottom curve) and 2[3] (top curve) sites for 1 year of the EMCD Viking dust scenario [7]

C. *Topology and Geology*

The mapping of the radiation environment of a planet based on σ layer calculations is highly dependent on its topology. For that reason the interface extracts the Martian surface altitude from the MOLA instrument on board NASA's Mars Global Surveyor (MGS) spacecraft [8].
Mars' geology also plays a very important role in the radiation environment characterization. The Martian atmosphere, being of very low density (maximum values of the order of 10^{-2} kgm^{-3}), behaves as a "soft" medium for incoming energetic radiation, which is therefore able to reach the Martian surface. As a result there is an important contribution from secondary radiation particles generated and backscattered at the surface.
The average density of Mars' soil is about 3.75 g cm^{-3} and the mantle and crust bulk composition consist mainly of silicon dioxide and iron oxides [9]. Sub-surface water and ice, for which recent evidence has been produced, are expected to have an effect on backscatter properties, and they can easily be introduced later into the framework.

D. *Radiation Transport and Simulated cases*

The Monte-Carlo transport of 10^5 protons through the Martian atmosphere and surface has been incorporated into the simulation. Particles are generated at the top of a column of the atmosphere of 5º x 5º**.** All primary and secondary particles are tracked from the generation point until they are absorbed, "killed" or reach geometry tracking limits (generally meaning having lost most of their energy).
All simulated cases (Cases A to J) referred to in the subsequent sections are defined in Table I and Figure 3.
The simulated cases presented in this paper are located: a) in the cliff of Olympus Mons (MO) volcano; and b) Tyrrhena Paterae (TP), one of the three large, ancient, low relief broad mountain of volcanic origin that have developed along faults that surrounds Hellas Basins [9].

TABLE I
SIMULATED CASES

Case	Long [°E]	Lat [°N]	Name	Solar Longitude	Time[4] [Hours]	Depth [g/cm^2]
A	75	-7.5	(TP)	180°-210°	12	14.12
B	75	-12.5	(TP)	180°-210°	12	14.46
C	80	-7.5	(TP)	180°-210°	02	14.63
D	80	-7.5	(TP)	180°-210°	12	13.95
E	80	-7.5	(TP)	180°-210°	22	14.46
F	80	-12.5	(TP)	180°-210°	12	13.65
G	-105	22.5	(OM)	180°-210°	12	9.60
H	-140	22.5	(OM)	180°-210°	02	16.46
I	-140	22.5	(OM)	180°-210°	12	16.63
J	-140	22.5	(OM)	180°-210°	22	17.44

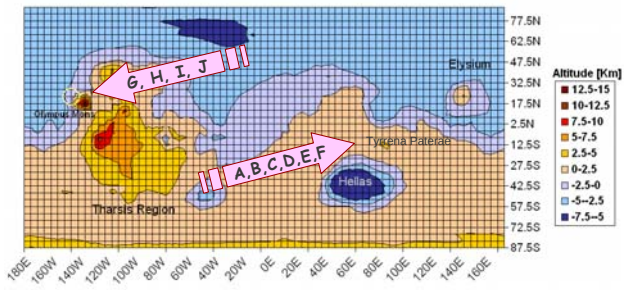

Figure 3-Simulated locations and the Martian map.

E. *Previous results*

Previous results already published [1][2] show GCR proton-induced fluences at the surface of the order of the 10^7 particles/cm^2 and that the induced radiation environment at the surface is highly dependent on the atmospheric pressure at the surface.

[2] Viking lander 1 was situated at 22ºN, 48ºW.
[3] Viking lander 2 was situated at 48ºN, 226ºW.
[4] Mars Universal time at Longitude 0º.

II. GCR-INDUCED RADIATION ENVIRONEMNT

In this paper a quantification diurnal and seasonal variations in the GCR proton-induced fluences at the surface of Mars is included.

Tables II and III show that while diurnal variations are of the order of 1% or lower, seasonal changes are of the order of 10 to 20%. Tables also show that an increase of the primary spectra at the surface is complemented by an increase in the fluence of neutrons and photons and a decrease of electrons and ions and others. This observation can be easily explained by the fact that neutrons and photons (detected at the surface) are mostly created by primary particles interaction with the surface while electrons, ions and other particles are mostly due to the interactions and spallation in the atmosphere. This conclusion is supported by results published in previous papers [1][2].

TABLE II
DIURNAL CHANGES AT LONGITUDE 0°: FLUENCES DUE TO GCR

Time		02	12	22	Max-Min
Particles Species		Fluence per year [x10^7 #/cm^2]	Fluence per year [x10^7 #/cm^2]	Fluence per event [x10^7 #/cm^2]	Relative difference [%]
Protons	Primary	3.549	3.553	3.557	0.23
	Secondary	0.5435	0.5412	0.5386	-0.91
Electrons		0.9717	0.9706	0.9693	-0.25
Neutrons		19.72	19.74	19.76	0.20
Photons		20.08	20.06	20.04	0.20
Other		1.723	1.718	1.712	0.64

TABLE III
SEASONAL CHANGES AT 12:00 HOURS AT LONGITUDE 0°
FLUENCES DUE TO GCR

LS		60°-90°	150°-180°	240°-270°	Max-Min
Particles Species		Fluence per year [x10^7 #/cm^2]	Fluence per year [x10^7 #/cm^2]	Fluence per event [x10^7 #/cm^2]	Relative difference [%]
Protons	Primary	3.450	3.604	3.425	5
	Secondary	0.6002	0.5117	0.6145	-18
Electrons		1.000	0.9559	1.007	-5
Neutrons		19.09	19.97	18.91	5
Photons		20.50	19.84	20.61	-4
Other		1.850	1.651	1.883	-13

III. GCR-INDUCED EFFECTS

Previously published results [1][2] show that while total ionizing doses at the surface of Mars are of lesser concern to EEE components, the relative abundance of protons and neutrons may result in Displacement Damage and Single Event Effects (SEEs) and Dose Equivalents (DEq) may reach critical values for manned missions.

The following subsections discuss the developed radiation-induced effects modules concerning the evaluation of SEEs and DEq.

A. Single Event Effects

The development of the Single Event Upset (SEU) Radiation Effects Module is based on the 4-Mbit ATMEL AT60142F SRAM devices comprehensively characterized as part of ESA's SEU reference monitor development activity [13]. The memory device's SEU cross-section data has been obtained for heavy ions, protons and neutrons. Several fit-functions described in the literature [8][9] were selected as candidates to represent the measured SEU cross-section data. Detailed study involving simulation work (using GEANT4 and CREME96) and validation combined with experimental data was carried out in order to identify the best fit-function for the ATMEL device's ion, proton and neutron SEU cross-section data. Different function parameters in particular the different SV thicknesses were simulated and results were compared. The study concluded that for this memory device the best-fit method was obtained employing the Weibull function [8].

The methodology may be easily adapted for implementation of other memory devices.

Results illustrated in this paper refer to 1.5 μm SV thickness.

Figure 4 illustrates the MarsREC reconstruction of the SEU cross-section as a function of particle energy for protons and neutrons and compares these with experimental data.

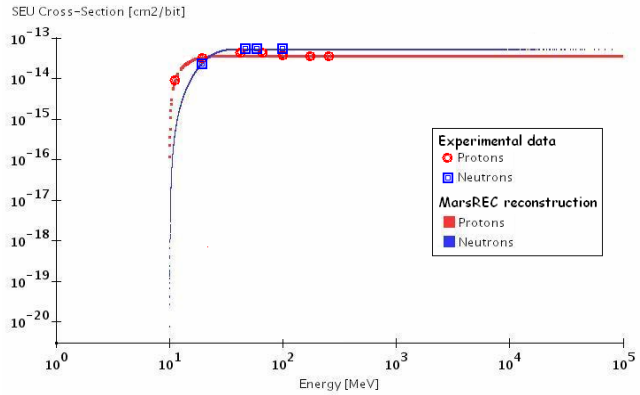

Figure 4- SEU cross-sections for protons and neutrons: MarsREC reconstruction and experimental data.

1) Principle of SEU Rate Calculation

SEUs may be induced directly by heavy ions and indirectly by protons and neutrons with energies ranging from a few MeV to more than some GeV. The physical mechanism responsible for inducing SEUs is different for ions and for protons and neutrons. In this extended abstract results only focus on indirect induced SEUs by protons and neutrons.

In the SEU Radiation Effects Module the upset rate for incident protons or neutrons, N, is given as a function of particle flux and SEU cross section:

$$N_{\substack{\text{Protons}\\ \text{Neutrons}}} = \int_{E_{\min}}^{E_{\max}} \frac{d\phi}{dE}(E)\cdot\sigma_p(E)\cdot dE \qquad (1)$$

where dϕ/dE is the differential energy spectrum, $\sigma_p(E)$ is the proton upset cross section, E_{min} and E_{max} are the minimum and maximum energy of the differential energy spectrum [10]-[13].

Table IV shows the total SEU rates expected per device in one year.

TABLE IV

Particles	SEU Rates one year [#/Device]
Protons	4.98
Neutrons	2.21

After normalization corrections between different models, MarsREC results simulated with perpendicular and isotropic incident beams were compared with CREME96 [10][11], as illustrated in Figure 5. It can be seen that results obtained with a perpendicular incident beam are closer to CREME96 results. This result can be easily understood once CREME96 simulates a spherical-concentric geometry. This geometry is comparable in a first approach to infinite slab geometry with perpendicular incident beam. On the other hand an increase of the difference between MarsREC (perpendicular) and CREME96 can be seen for increasing depth values. This is explained by the fact that GEANT4 is a Monte Carlo tool that allows the generation of secondary particles in all 3D directions and so increasing the depth the pass length of all product of interaction is increased by a cosine factor not considered in CREME96.
Finally Figure 5 shows that MarsREC results are in very good agreement with CREME96 predictions under similar geometric conditions.

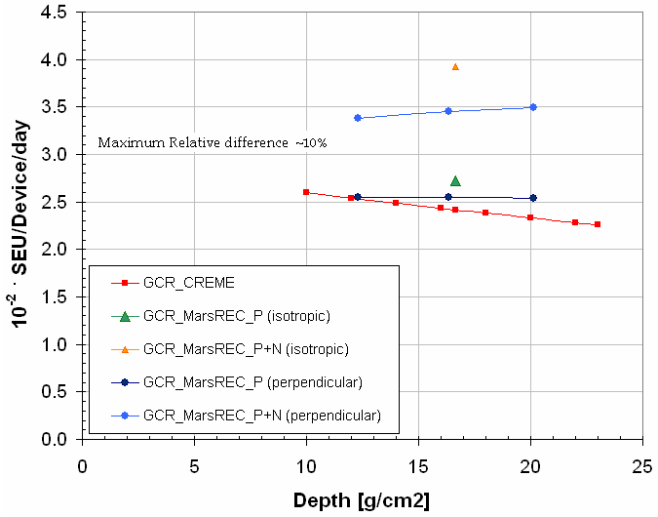

Figure 5- GCR- induced SEU rates predictions with MarsREC and CREME 96.

B. *Dose Equivalent*

Most of the published studies concerning the effects of radiation in manned missions for space exploration, present results in units of dose equivalent.
According to the ICRU (International Commission on Radiological Units and Measurements) [14][15][16] the dose equivalent is the product of the absorbed dose at a given LET in tissue, and a weighting factor for that LET. The special name for the unit of dose equivalent is sievert (Sv)[5].
The MarsREC post-processing module for dose equivalent calculation consists of the use of FLUKA fluence-to-ambient dose equivalent conversion coefficients [17][18].
As described in literature FLUKA fluence-to-ambient dose equivalent conversion coefficients, $f_{H^*(E)}$, were calculated in terms of ambient dose equivalent, *H*(E)*, per unit of fluence (Sv.cm2):

$$f_{H^*(E)} = \frac{H^*(E)}{\Phi(E)} \text{ . [13-14]} \qquad (2)$$

where $\Phi(E)$ is the fluence of primary particle of energy E.
Macro files have been created to evaluate the fluences of particles in the energy ranges identified by FLUKA [17][18] for protons, neutrons, electrons and photons. This macro files were run for all the simulated cases illustrated in Table I.
After fluences were computed for each kind of particles, i, conversion factors were multiplied by the fluences as illustrated in equation 3, to obtain the ambient dose equivalent, $H_i{}^*(E)$.

$$H_i{}^*(E) = f^{\,i}{}_{H^*(E)} \cdot \Phi_i(E) \qquad (3)$$

Then for each kind of particle the total dose equivalent, H_i, was obtained by adding the contributions from all energy ranges

$$H_i = \sum_E f^{\,i}{}_{H^*(E)} \cdot \Phi_i(E) \qquad (4)$$

Finally the total ambient dose equivalent, *H*, was obtained by adding all the contributions from the different particles.

$$H = \sum_i H_i \qquad (5)$$

FLUKA does not give conversion factors for ions. For this reason two approaches have been hold: 1st. Not considering ions contribution since their total fluence is much lower than the other particles'; 2nd. According to ICRU publications [14] protons' weighting factor is 5, while the weighting factor for Alpha particles, fission fragments and heavy nuclei is 20. Therefore Ions were considered to have proton similar fluence-to-dose equivalent conversion multiplied by four.
Figure 6 shows MarsREC converted Dose Equivalents both with and without ions (blue and magenta triangles) and MARIE (NASA Mars Radiation Environment Experiment) software predictions (red dot)[19]. It can be seen that the maximum relative difference is obtained for the total Dose Equivalent considering the MarsREC conversion for all particles including ions and it is as much as 3%.

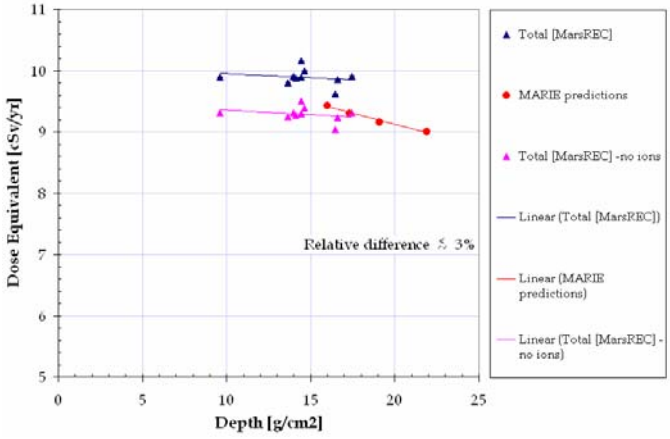

Figure 6- Dose Equivalents.

[5] 1Sv=1 J kg^{-1}.

C. *Verification*

Table V summarizes and quantifies the comparisons described in sections A and B.

TABLE IV [19] [20]

MODEL	DEPTH [g/cm^2]	DOSE EQUIVALENT [cSv/yr]	SEU 10^{-2}[#/device/day]
MARSREC	17.4	9.25	2.57
	16.7	9.26	2.72
MARIE	17.3	9.3	----------
CREME96	16.7	----------	2.42

IV. CONCLUSIONS

MarsREC is an integrated simulation tool for Mars Radiation Environment and Radiation Characterization and induced Effect. It consists of three modules: two pre-processing modules providing a comprehensive method for Radiation Environment and SEU Rate prediction for EEE components on Mars; and a post-processing module for dose Equivalent calculations based on FLUKA fluence-to-ambient dose equivalent conversion coefficients. Results show that the developed framework is capable of calculating the energy spectra and particle species, radiation fluxes at component level, energy depositions doses, dose equivalents as well as predicting SEU rates for protons and neutrons.

MarsREC results show very good agreement when compared with other software's predictions.

V. ACKNOWLEDGMENTS

This work was funded by the Portuguese Foundation for Science and Technology and by the European Space Agency

VI. REFERENCES

[1] A.Keating et all, Mars Atmosphere Modeling & Observation Workshop, Granada 2006. Available:http://www-mars.lmd.jussieu.fr/granada2006/abstracts/Keating_Granada2006.pdf

[2] A.Keating, et al, "A Model for Mars Radiation Environment Characterization", *NSREC*, Seattle, USA, 12th July, 2005 (accepted to IEEE-TNS).

[3] L. Desorgher, "Planetocosmics GEANT4,", http://cosray.unibe.ch/%7Elaurent/planetocosmics/ , Jul. 4, 2005.

[4] S Agostinelli et al, "Geant4-A simulation toolkit", *Nucl Instrum Meth Phys Res.*, A506, Issue 3, 2003, pp. 250-303.

[5] J. Allison et al, "Geant4 Developments and Applications", *IEEE TNS* Vol. 53, no. 1, February 2006, pp-270-278.

[6] F.Forget. (2001, May 18). *What is the Mars Climate Database?* Avilable: http://www-mars.lmd.jussieu.fr/

[7] S.R.Lewis, M.Collins, and P.L.Read, "A climate database for Mars", *Journal of Geophysical Research–Plane*ts, vol. 104, no. E10, pages 24,177–24,194 (1999).

[8] James B. Abshire, Xiaoli Sun, Robert S. Afzal. (1999, August). Mars Orbiter Laser Altimeter Receiver Model and Performance Analysis. *NASA Goddard Space Flight Center Laser Remote Sensing Branch*. Available: http://pds-geosciences.wustl.edu/geodata/mgs-m-mola-3-pedr-l1a-1/mgsl_21xx/document/calib.pdf

[9] Joseph M. Boyce, *The Smithsonian Book of Mars*, Smithsonian Institution Press, 2002, 88-125.

[10] A.J.Tylka (2003, December 15). *Orbit Selection on CREME96 for Flux*. Available: https://creme96.nrl.navy.mil/cm/FluxOrbit.htm

[11] A.J.Tylka et al, "CREME96: A revision of the Cosmic Ray Effects on Micro-Electronics Code", *IEEE Transitions on Nuclear Science*, 1997, vol. 44, pp.2150-2160.

[12] ESA. (2005, August 4). *Aurora Exploration Program*. Available: http://www.esa.int/SPECIALS/Aurora/SEM1NVZKQAD_0.html.

[13] R. Harboe- Sørensen, F.-X. Guerre and A. Roseng, "Design, Testing and Calibration of a **Reference SEU Monitor** System, proceedings, RADECS 2005

[14] International Commission on Radiological Protection, 1990 Recommendations of the International Commission on Radiological Protection, ICRP Publication 60, Annals of ICRP, 21(1-3) (1991).

[15] Pelliccioni, M. Radiation Weighting Factors and Conversion Coefficients for High- Energy Radiation, SATIF-4, Workshop Proceedings Knoxville, 17-18 September 1998, 179-192, OECD (1999).

[16] Kramer R., Zankl M., Williams G. and Drexler G. The Calculation of Dose from External Photon Exposure Using Reference Human Phantoms and Monte Carlo Methods. Part I: The Male (ADAM) and Female (EVA) Adult Mathematical Phantoms. Neuherberger, GSF-Forschungszentrum für Umweit und Gesundheit, GSF-Bericht S885 (1982).

[17] M. Pelliccioni, "Conversion coefficients for high-energy radiation calculated using the FLUKA Code", [Online] G.Battistoni (2003-05-09) http://www.mi.infn.it/~battist/DoseCoeff/node3.html

[18] Pelliccioni, M.,"Overview of Fluence-to-Effective Dose and Fluence-to-Ambient Dose Equivalent Conversion Coefficients for High Energy Radiation Calculated Using the FLUKA Code", Radiat. Prot. Dosim. 88(4), 279-297 (2000)

[19] F.A. Cucinotta, C. Dardano (27th October 2003), "MARIE, Mars Radiation Environment Experiment: References and Documents", online: http://marie.jsc.nasa.gov/Documents/Index.html

[20] J.W.Wilson, J.Miller, A.Konradi and F.A. Cucinotta, "Shielding Strategies for Human Space Exploration", NASA Conference Publication 3360, December 1997.